

Mitochondrial Genome Deletion Aids in the Identification of False- and True-Negative Prostate Needle Core Biopsy Specimens

Jennifer Maki,^{1*} Kerry Robinson, MSc,^{1*} Brian Reguly,^{1*} Jude Alexander, MSc,^{1*} Roy Wittcock, MSc,^{1*} Andrea Aguirre, MSc,^{1*} Eleftherios P. Diamandis, MD, PhD,² Nicholas Escott, MD,³ Anthony Skehan, MD, PhD,⁴ Owen Prowse, MD,⁴ Robert E. Thayer, PhD,^{1*} M. Kent Froberg, MD,⁵ Michael J. Wilson, PhD,⁶ Samantha Maragh,⁷ John P. Jakupciak, PhD,⁸ Paul D. Wagner, PhD,⁹ Sudhir Srivastava, PhD,⁹ Gabriel D. Dakubo, MB, ChB,^{1*} and Ryan L. Parr, PhD^{1*}

Key Words: mtDNA deletion; Prostate biopsy; False-negative biopsy result; Sensitivity; Specificity; Field cancerization

DOI: 10.1309/UJJTH4HFEPWAQ78Q

Abstract

We report the usefulness of a 3.4-kb mitochondrial genome deletion (3.4mtΔ) for molecular definition of benign, malignant, and proximal to malignant (PTM) prostate needle biopsy specimens. The 3.4mtΔ was identified through long-extension polymerase chain reaction (PCR) analysis of frozen prostate cancer samples. A quantitative PCR assay was developed to measure the levels of the 3.4mtΔ in clinical samples. For normalization, amplifications of a nuclear target and total mitochondrial DNA were included. Cycle threshold data from these targets were used to calculate a score for each biopsy sample. In a pilot study of 38 benign, 29 malignant, and 41 PTM biopsy specimens, the difference between benign and malignant core biopsy specimens was well differentiated ($P < .0001$), with PTM indistinguishable from malignant samples ($P = .833$). Results of a larger study were identical. In comparison with histopathologic examination for benign and malignant samples, the sensitivity and specificity were 80% and 71%, respectively, and the area under a receiver operating characteristic (ROC) curve was 0.83 for the deletion. In a blinded external validation study, the sensitivity and specificity were 83% and 79%, and the area under the ROC curve was 0.87. The 3.4mtΔ may be useful in defining malignant, benign, and PTM prostate tissues.

The unique maternal inheritance pattern of mitochondrial DNA (mtDNA), its small genome size, lack of recombination during gametogenesis, and multiple copy number per cell, in comparison with nuclear DNA, identify this molecule as important and economical to characterize at a population level. It is well known that mitochondria are important participants in cellular function. Not only does the machinery of this organelle produce up to 90% of required cellular energy, it also has a critical function in mediated cell death through the apoptotic pathway.¹⁻³ Moreover, mitochondria modulate appearance, copy number, and location during the cell cycle.⁴

These characteristics suggest that mitochondria may undergo detectable modifications associated with malignant progression. In particular, mitochondria have been implicated in the carcinogenic process, partly because of their role in apoptosis and other aspects of tumor biology.⁵ Damage accrued by the mitochondrial genome (mtgenome) is associated with increased cellular stress and organelle dysfunction.⁶ Indeed, numerous studies have identified somatic mutations in this modest genome.⁷ Several groups have demonstrated mtgenome alterations in many cancers.^{8,9} Studies of mtDNA alterations in prostate cancer (PCa) indicate the presence of mutations in the prostate, probably as a result of increased reactive oxygen species production in the glandular epithelial tissues.^{10,11}

Not only does the modest mtgenome code for 13 proteins, which participate in the electron transport chain as well as 22 transfer RNAs (tRNAs) required for transcription of these genes and 2 ribosomes (12SrRNA and 16SrRNA), but it is also saturated with direct repeats that flank deletions, a common mutation genre of this genome, in addition to point mutations. Many mitochondrial myopathies are characterized by

mtgenome deletions.¹² Specifically, much work has been done on a 4,977-base-pair (bp) or “common deletion.” This portion of the mtgenome has been deleted in many pathologic conditions, including cancer. It is important to note that deletions in the mtgenome have been reported in PCa and might mediate androgen independence,^{13,14} although one study could not identify mtDNA deletions in these tumors.¹⁵

An irregular result from a digital rectal examination (DRE) and/or elevated prostate-specific antigen (PSA) level in the blood generally triggers referral to the urologist for a prostate biopsy procedure. In most cases, the results are negative for malignancy, which is clinically problematic because some of the patients continue to have abnormal PSA and DRE findings. Indeed, about 10% and 5% will have PCa on second and third repeated biopsy procedures.¹⁶ An obvious concern with the use of histopathologic examination for identifying malignant disease is that this method relies on cell morphologic features rather than molecular indications.¹⁷ Because neoplasia and the potential cellular transformation to malignancy are based on alterations in gene function, changes in cell appearance occur relatively late in this process. In contrast, mtgenome mutations may occur early in the transformation process.¹¹ Thus, a biomarker that can predict a missed tumor in prostate biopsy specimens will be a useful complement in evaluation of prostate biopsy samples. We describe the discovery and characterization of a 3.4-kb mtgenome deletion (3.4mtΔ) that has high statistical association with PCa. It is important to note that this 3.4mtΔ demonstrates a field cancerization, which may have usefulness as an adjunct in evaluation of prostate biopsy specimens.

Materials and Methods

Patients and Sample Criteria

Ethics

All samples were obtained in accordance with the ethical guidelines of the Thunder Bay Regional Hospital Ethics Board (Thunder Bay, Canada) and the Trafalgar Ethics Board (Oakville, Canada). Both boards operate in accordance with the Tri-Council Policy Statement on Ethical Conduct for Research Involving Humans.

Pilot Study

We used 38 benign biopsy specimens from 22 patients (average age, 66 years), 41 malignant biopsy specimens from 24 patients (average age, 68 years; mostly Gleason 6/7), and 29 proximal to malignant (PTM) biopsy specimens from 22 patients (average age, 71 years). All patients with malignant biopsy specimens had a follow-up prostatectomy to confirm

diagnosis of PCa, and the PTM samples were negative biopsy specimens from this cohort. Malignant and PTM core needle biopsy samples were selected after a review of a pathology report associated with a radical prostatectomy. Benign samples were selected based on a single negative biopsy result.

Confirmation Study

For this study, we used 98 benign biopsy specimens from 22 patients (average age, 62 years), 75 malignant biopsy specimens from 65 patients (average age, 67 years), and 123 PTM biopsy specimens from 96 patients (average age, 67 years). Samples were selected based on biopsy pathology reports in an effort to mimic typical clinical samples. To ensure benign tissue status, patients were required to have at least 2 successive negative biopsy procedures, with biopsy specimens from the first procedure used for analyses. Malignant samples were screened by a qualified pathologist (N.E.), and most were Gleason score 6 or 7. PTM samples were defined as histopathologically normal biopsy specimens adjacent to a malignant needle core specimen.

DNA Extraction and Target Amplification

Nucleic acids from frozen (50 mg) and formalin-fixed, paraffin-embedded (FFPE) prostate needle biopsy (20-μm sections) samples were extracted using a QIAamp DNA Mini Kit (Qiagen, Mississauga, Canada). Negative extraction control samples were processed in parallel with biopsy tissues and monitored for amplification. Extracts were quantified by using a NanoDrop ND-1000 Spectrophotometer (NanoDrop Technologies, Wilmington, DE). Before amplification, samples were diluted to 2 ng/μL and distributed to master template 96-well plates. Templates from the 96-well plates were amplified using iQ Sybr Green Supermix (Bio-Rad Laboratories, Hercules, CA).

Reaction conditions were as follows: 1× iQ Sybr Green Supermix, 0.25 μmol/L of forward primer, 0.25 μmol/L of reverse primer, and 20 ng of template DNA in a 25-μL reaction volume. Cycling parameters were 95°C for 3 minutes, followed by 45 cycles of 95°C for 30 seconds, 30 seconds annealing at optimized primer temperatures (61.5°C for total mtDNA and tumor necrosis factor [TNF], 66°C for deletion-specific primer), and extension at 72°C for 30 seconds. Each extension was followed by a plate reading. A 10-minute final extension at 72°C was performed before the melting curve (50°C to 105°C, reading every 1°C and holding for 3 seconds). Cycling was performed on a DNA Engine Opticon 2 Real-Time PCR (polymerase chain reaction) Detection System (Bio-Rad Laboratories). One negative PCR control sample was included on every amplification plate for each primer set, as were 6 standards for normalization purposes. These standards were serial dilutions of the target amplicon generated with conventional PCR, purified, quantified, and diluted such

that the 6 standards were at the following concentrations: 3.85 ng, 0.385 ng, 38.5 pg, 3.85 pg, 0.385 pg, and 38.5 fg. A minimum of 4 standards was used in the analysis of any given plate.

Long-range PCR was performed in a 50- μ L reaction volume containing 50 ng of template, 0.4 mmol/L each of deoxynucleoside triphosphates, 0.5 U/ μ L of LA *Taq* polymerase, 0.2 μ mol/L of primers and 1 \times LA buffer. The cycling conditions were 94°C for 1 minute followed by 30 cycles consisting of 94°C for 10 seconds and 68°C for 15 minutes, followed by a final extension at 72°C for 10 minutes.

Statistical Analysis

The cycle threshold (C_t) of the 3.4mt Δ was compared with the C_t of 2 additional targets designed to capture the total amount of mtDNA (12SrRNA gene) and the amount of nuclear DNA (single-copy *TNF*). Cycle thresholds of all 3 targets were used in a simple formula [$C_t^{\text{del}} - C_t^{\text{tot}}/C_t^{\text{tnf}}$], which provides a score for each sample. This score is hereafter referred to as the residual mtDNA score or RM score. The mean and SD were calculated for each tissue classification, as were mean and 99% confidence intervals (CIs). A 1-way analysis of variance was used to test for statistical significance between groups.

Results

Full-length mtgenome amplification of frozen malignant prostate tissues identified a 3,379-bp deletion (deletion junction 10744:14124) in PCa **Figure 1**. This large-scale deletion removes the terminal 22 bases of ND4L, all of ND4, 3 tRNAs (histidine, serine 2, and leucine 2), and all except the terminal 24 bases of ND5.¹² Initial analysis of 33 frozen PCa samples revealed the presence of this deletion in 30 (91%) of 33 samples **Figure 2B**. Sequencing of the PCR product was performed to confirm its mitochondrial origin.

The association of this deletion with PCa could not be determined without normal control samples, which were not available for the frozen samples; therefore, we redesigned PCR primers targeting a smaller amplicon from this deletion to study FFPE biopsy specimens for which control samples were available. To achieve this, a new reverse primer was combined with the deletion-specific forward primer **Figure 2A** (primer set 2 and 3) to yield an amplicon of 272 bp. These primers failed to amplify template from p^0 cells **Figure 2G**. By using this primer pair, we performed a qualitative PCR on 4 PCa samples, 2 of which had PTM samples as well. Interestingly, the deletion was present in all samples **Figure 2C**. Further analysis of FFPE biopsy samples confirmed the presence of the deletion in malignant and PTM samples, but it was virtually absent in benign samples **Figure 2D** and

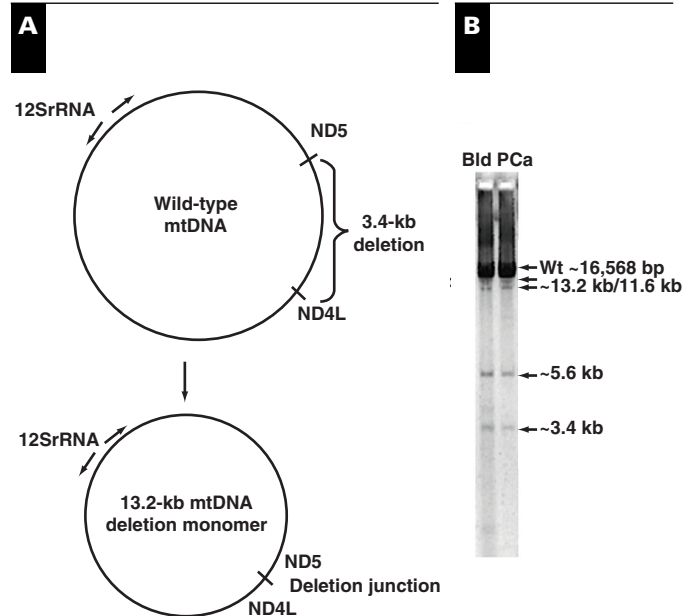


Figure 1 Long-extension PCR (LXPCR) identified a 3.4-kb deletion (appears on gel as 13.2-kb deletion band). **A**, Primer locations, deletion breakpoints, and the 13.2-kb recircularized mitochondrial genomes are shown. **B**, A gel picture of LXPCR on template from prostate cancer (PCa) and blood (Bld) depicts the wild-type band and deleted molecules (low-molecular-weight bands), which include the 13.2-kb band and the common deletion (appears as 11.6-kb band). mtDNA, mitochondrial DNA; rRNA, ribosomal RNA.

Figure 2E. As a further authentication of the mitochondrial origin of the PCR product, we performed restriction analysis on the amplicon using *AluI* and *BamHI*, and the expected product sizes were obtained **Figure 2F**.

By using the 272-bp PCR primers, a quantitative PCR was developed to closely monitor the association of this deletion with PCa. For quantitative determination of the levels of the 3.4mt Δ in clinical samples, 2 control primers were included; a primer pair located in a minimally deleted mtDNA region (12SrRNA) was used to amplify total mtDNA as a control for mtDNA copy number within each extract, and a primer set targeting a single-copy nuclear gene (*TNF*) was used to control for cellular copy number **Table 1**. Normalized C_t s from 39 malignant and 41 benign samples were statistically analyzed. C_t s for benign and malignant samples were significantly different for the deletion, but not for total and *TNF*. In view of this, using the 3 C_t parameters in computing the RM score for each sample was justified.

For it to be of value in PCa detection, the 3.4mt Δ should not be associated with other common benign prostatic conditions such as benign prostatic hyperplasia, prostatic atrophy, and inflammation. As shown in **Figure 3A**, the RM scores of

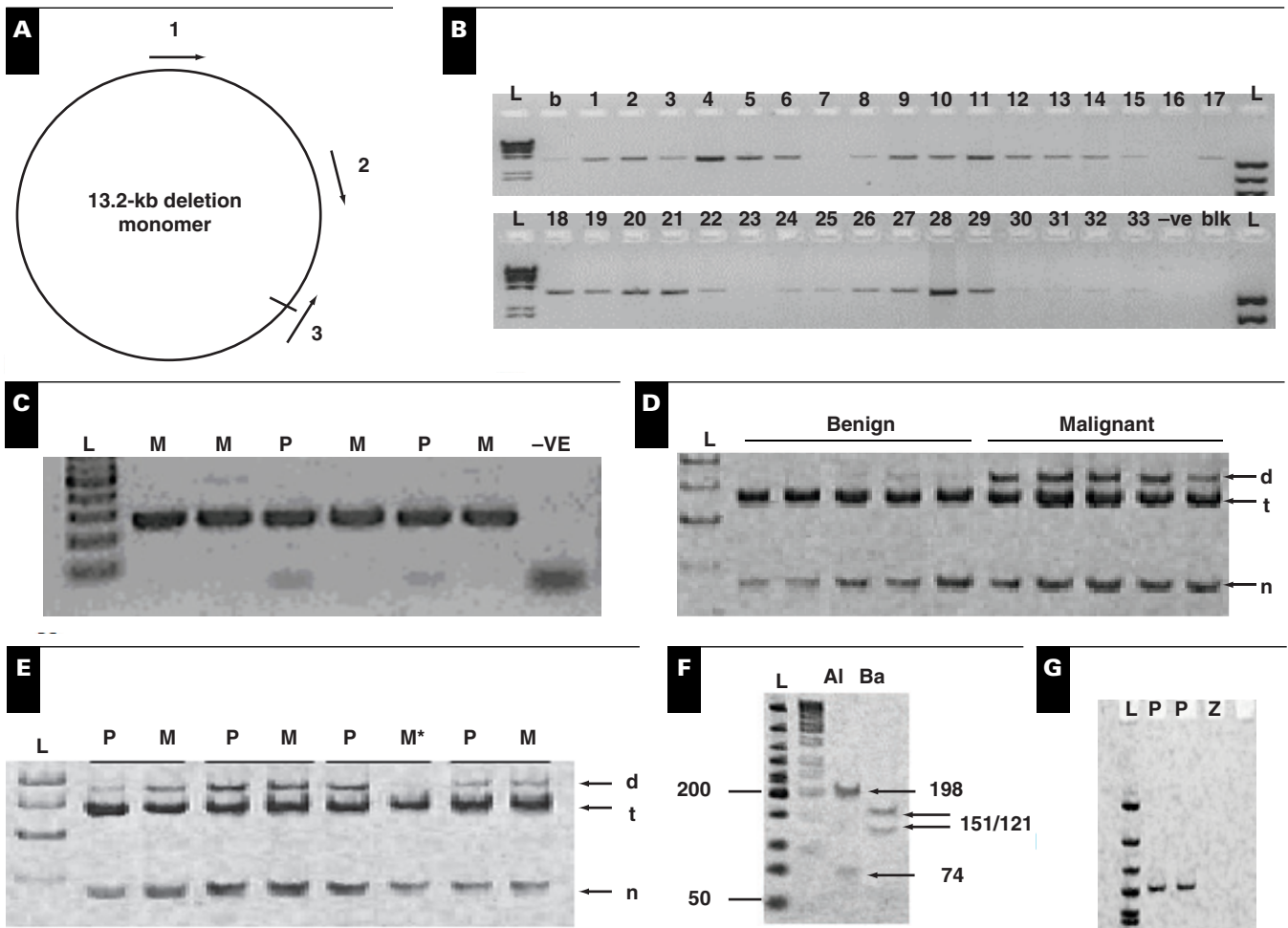


Figure 2 Initial analysis of prostate cancer samples for the 3.4-kb mitochondrial genome deletion (3.4mtΔ). **A**, Locations of primers used for screening and quantitative polymerase chain reaction (PCR) assay development. **B**, Initial screening of 33 prostate cancer samples with primer pair 1 and 3 shows the presence of the 3.4mtΔ in 30 samples. b, blood; -ve, PCR negative control; blk, blank well. **C**, Analysis of frozen malignant prostate (M) and proximal to malignant (PTM) (P) samples with primer set 2 and 3 reveals the presence of the 3.4mtΔ in PTM samples as well. **D** and **E**, Screening of benign, malignant (M), and PTM (P) formalin-fixed, paraffin-embedded biopsy samples demonstrates the virtual absence of the 3.4mtΔ (d) in benign samples (**D**). Amplification of total (t) and TNF (n) targets were included in these runs. *This is probably a failed PCR reaction. **F**, Restriction analysis of the 272-base-pair PCR product with *AluI* (Al) and *BamHI* (Ba) authenticate its mitochondrial origin. **G**, Amplification of template from p⁰ (Z) and prostate (P) indicates absence of amplification of nuclear mitochondrial DNA targets.

Table 1
Primer Descriptions

Primer Name	Primer Location	Primer Sequence (5'-3')
Total		
Forward	708-728	cgttccagtgagttcaccctc
Reverse	923-945	cactctttacgccggtctctatt
TNF		
Forward	906-925	cctgccccaatccctttatt
Reverse	1016-1036	ggtttcgaagtgggtgctctg
3.4-kb Deletion		
Forward	10729-10743/ 14125-14139	tagactacgtacataacctaaccctactccta
Reverse	14361-14379	gaggtaggattgggtgctgt
LXPCR		
Forward	1135-1159	ccagaacactacgagccacagctta
Reverse	1050-1077	atcccagttgggtcttagctattgtg

LXPCR, long-extension polymerase chain reaction; TNF, tumor necrosis factor.

benign prostatic conditions indeed cluster with normal benign samples and are distinctly separate from malignant samples. This demonstrates that the 3.4mtΔ is associated with PCa and, thus, might be of value in PCa detection. In addition, preliminary analysis of 8 samples of prostatic intraepithelial neoplasia demonstrated that 5 of 8 were malignant (Table 2). It should be noted that microdissection was not performed, and, therefore, more work is required to reveal the behavior of this biomarker in pure prostatic intraepithelial neoplasia samples and in other “suspicious” malignant lesions.

Our analysis of frozen samples indicated the presence of the 3.4mtΔ in histologically normal samples in proximity to

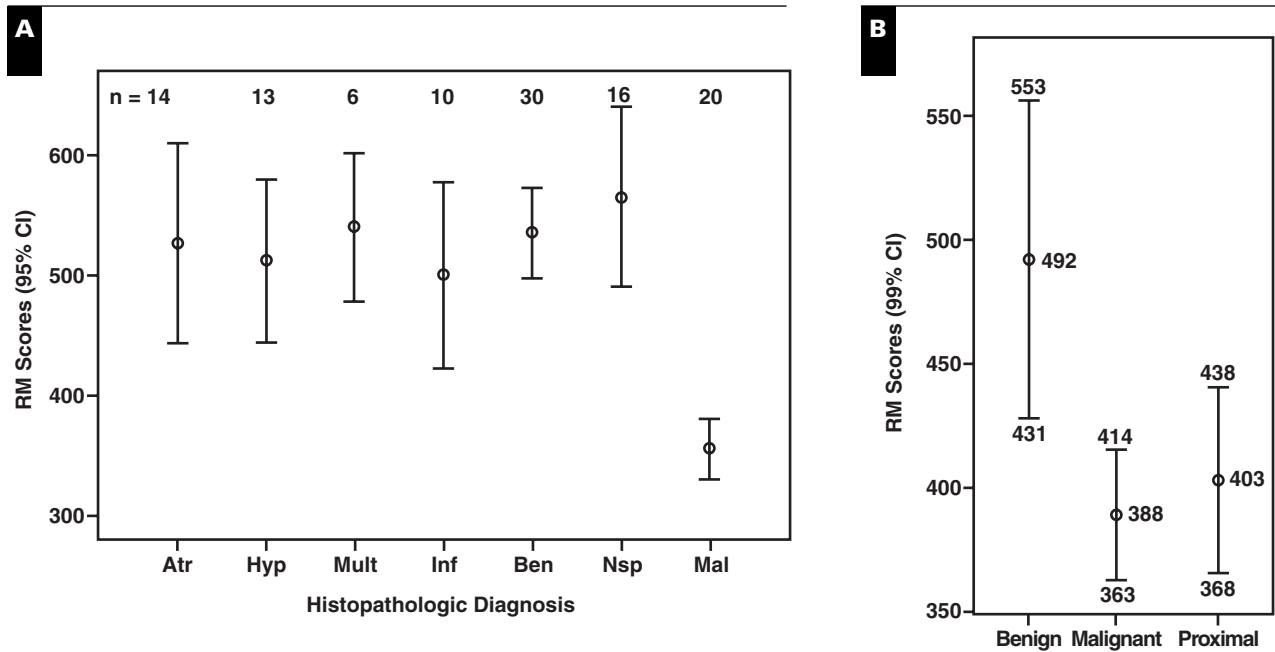


Figure 3 **A**, The 3.4-kb mitochondrial genome deletion is associated with prostate cancer. The mean residual mitochondrial DNA (RM) scores and 95% confidence intervals of benign prostatic conditions (Atr, atrophy; Ben, benign without other lesions; Hyp, hyperplasia; Inf, inflammation; Mult, multiple prostatic lesions; Nsp, nonspecific benign changes) and prostate cancer (Mal) are plotted. Above each plot is the number of samples analyzed. **B**, The deletion demonstrates a field cancerization effect. Plots of the mean RM scores and 99% confidence interval (CI) of the pilot studies for benign, malignant, and proximal samples are shown. Note how closely the RM scores of the proximal samples resemble the malignant samples. It is also noteworthy that the 99% CI of the benign samples is extremely vast, which is likely because these samples were from single benign biopsy procedures, some of which might already be demonstrating the field cancerization effect.

PCa, suggesting that this deletion demonstrates a cancer field effect. This observation is of interest because it may be of complementary value in the evaluation of false-negative biopsy results. To evaluate this aspect further, a pilot study was conducted using biopsy specimens from 46 patients (Table 3). The RM scores were statistically significant between benign and malignant ($P < .0001$) and benign and proximal ($P < .003$) samples. Consistent with the field cancerization phenomenon observed in the frozen samples, the PTM samples closely resembled the malignant samples, with no statistical significant resolution between their RM scores ($P < .833$). The mean and 99% CI for the RM scores for benign, malignant, and proximal samples are shown in Figure 3B.

Statistical parameters from the preceding data were used in a power calculation to determine the number of samples required for a blinded confirmation study to assess the robustness and reproducibility of the association of the 3.4mt Δ with PCa. The accuracy of the RM scores in predicting benign and malignant samples with reference to histopathologic examination (the “gold standard”) was determined using an RM score cutoff of 450 and also computation of a receiver operating characteristic (ROC) curve. The sensitivity and specificity were 80% and 71%, respectively,

Table 2
Behavior of the 3.4mt Δ in PIN Samples

Patient ID No.	Age (y)	Histopathologic Diagnosis	Prediction by 3.4mt Δ
833	68	1 or 2 foci of LPIN; <5%	Malignant
1152	78	Features of PIN	Malignant
292	75	Focal LPIN	Malignant
789	73	Focal PIN	Malignant
787	75	Tiny focal area of HPIN; <5%	Benign
1093	79	Focal PIN	Benign
646	65	PIN	Benign
1053	60	HPIN	Malignant

HPIN, high-grade PIN; LPIN, low-grade PIN; PIN, prostatic intraepithelial neoplasia; 3.4mt Δ , 3.4-kb mitochondrial genome deletion.

and the area under the ROC curve was fairly good, at 0.77 for the RM scores and 0.83 for the deletion Ct (Figure 4A). Again, there was a statistically significant difference in the RM scores between benign and malignant samples ($P < .0001$). Unlike the pilot study, the RM scores of the proximal samples from the blinded confirmation study were significantly different from malignant ($P < .001$) and benign ($P < .006$) groups. Figure 4B shows the mean RM

Table 3
Clinicopathologic Data for Patients in the Pilot Study

Patient ID No.	Age (y)	PSA (ng/mL)*	DRE	Histopathologic Diagnosis (Gleason Grade)	3.4mtΔ Prediction	% of Core Positive
1004B	77	NR	NR	Malignant (3 + 3 = 6/10)	Malignant	20
1004C				Benign; PTM	Malignant	
1005B	84	NR	NR	Benign; PTM	Malignant	
1005E				Malignant (3 + 3 = 6/10)	Malignant	15
1023A	77	NR	NR	Malignant (3 + 4 = 7/10)	Malignant	60
1023F				Benign; PTM	Malignant	
1038A	59	NR	NR	Malignant (3 + 3 = 6/10)	Malignant	90
1038F				Malignant (3 + 4 = 7/10)	Malignant	80
1038G				Malignant (3 + 4 = 7/10)	Malignant	NR
1038H				Malignant (3 + 4 = 7/10)	Malignant	70
1041B	71	NR	NR	Benign; PTM	Malignant	
1041C				Malignant (3 + 3 = 6/10)	Malignant	10
1041H				Malignant (3 + 3 = 6/10)	Malignant	50
1041I				Malignant (3 + 3 = 6/10)	Malignant	20
1046I	61	NR	NR	Malignant (3 + 4 = 7/10)	Malignant	10
1047F	71	NR	NR	Malignant (3 + 3 = 6/10)	Malignant	25
1050F	73	NR	NR	Malignant (3 + 3 = 6/10)	Malignant	60
1054B	58	NR	NR	Benign; PTM	Malignant	
1054D				Malignant (3 + 3 = 6/10)	Malignant	15
1055A	66	NR	NR	Benign; PTM	Malignant	
1055D				Malignant (3 + 4 = 7/10)	Malignant	95
1055E				Malignant (3 + 4 = 7/10)	Malignant	75
1055F				Malignant (3 + 4 = 7/10)	Malignant	80
1061E	72	NR	NR	Benign; PTM	Malignant	
1062D	78	NR	NR	Malignant (3 + 3 = 6/10)	Malignant	NR
1062E				Benign; PTM	Malignant	
1084A	57	88	NR	Malignant (3 + 3 = 6/10)	Malignant	40
1091C	57	NR	NR	Benign; PTM	Malignant	
1091E				Malignant (4 + 4 = 8/10)	Malignant	5
1091F				Benign; PTM	Benign	
1105A	61	NR	NR	Malignant (3 + 3 = 6/10)	Malignant	50
1105C				Benign; PTM	Benign	
1105D				Malignant (3 + 3 = 6/10)	Malignant	NR
1105H				Malignant (3 + 3 = 6/10)	Malignant	60
1108H	64	NR	NR	Benign; PTM	Benign	
1108C				Malignant (3 + 3 = 6/10)	Malignant	5
1117B	86	NR	NR	Malignant (3 + 3 = 6/10)	Malignant	90
1117C				Malignant (3 + 3 = 6/10)	Malignant	80
1117E				Malignant (3 + 3 = 6/10)	Malignant	40
1117F				Malignant (3 + 3 = 6/10)	Malignant	100
1120D	64	NR	NR	Malignant (3 + 3 = 6/10)	Benign	5
1129D	73	NR	NR	Malignant (3 + 4 = 7/10)	Benign	10
1130E	57	NR	NR	Malignant (3 + 3 = 6/10)	Malignant	50
1131F	58	NR	NR	Malignant (3 + 3 = 6/10)	Malignant	30
1132E	71	NR	NR	Malignant (3 + 4 = 7/10)	Malignant	25
1148A	64	NR	NR	Malignant (3 + 4 = 7/10)	Malignant	40
1148D				Benign; PTM	Malignant	
1155A	83	5.93	NR	Benign; PTM	Benign	
1155D				Malignant (3 + 4 = 7/10)	Benign	30
1156D	76	NR	NR	Malignant (3 + 3 = 6/10)	Malignant	100
1156B				Benign; PTM	Malignant	
1156E				Benign; PTM	Malignant	
1167B	70	NR	NR	Malignant (3 + 4 = 7/10)	Malignant	100

DRE, digital rectal examination finding; NR, not recorded; PSA, prostate-specific antigen; PTM, proximal to malignant; 3.4mtΔ, 3.4-kb mitochondrial genome deletion. *Values are given in conventional units. To convert to Système International units (μg/L), multiply by 1.0.

scores and 99% CI for the benign, malignant, and proximal biopsy specimens.

For half of the patients (n = 48) who contributed proximal biopsy specimens for the confirmation study, we also obtained the corresponding malignant biopsy specimen for comparative analysis. In this patient category, the predictive accuracy of the RM scores of the proximal biopsy specimens

in correctly calling the presence of a malignant focus (ie, demonstrating field cancerization) was 67% (32/48). When 2 or more proximal biopsy specimens from the same patient were considered, the predictive power was 78% (14/18), suggesting that increasing the number of histologically normal biopsy specimens for analysis will increase the detection rate of the 3.4mtΔ.

Patient ID No.	Age (y)	PSA (ng/mL)*	DRE	Histopathologic Diagnosis (Gleason Grade)	3.4mtΔ Prediction	% of Core Positive
1167E				Benign; PTM	Malignant	
1170D	76	10	NR	Malignant (3 + 3 = 6/10)	Malignant	30
1170A				Benign; PTM	Malignant	
1186B	78	NR	NR	Malignant (3 + 4 = 7/10)	Malignant	50
1187B	70	NR	NR	Malignant (3 + 3 = 6/10)	Malignant	5
1187E				Benign; PTM	Malignant	
132E	79	5.9	35 cc	Benign	Benign	
136D	66	8.4	89 g	Benign	Benign	
270B	59	4.07	NR	Benign	Malignant	
270C				Benign	Malignant	
375B	64	6.13	NR	Benign	Benign	
51D	71	4.55	63 g	Benign	Benign	
536A	63	>5.25	472 cc	Benign	Benign	
560C	81	22.5	NR	Benign	Benign	
560D				Benign	Benign	
560E	81	22.5	0	Benign	Benign	
636F	68	9.35	91 g	Benign	Malignant	
637B	62	8.46	21 g	Benign; PTM	Malignant	
637E				Benign; PTM	Malignant	
638C	71	9.02	NR	Benign	Benign	
642A	61	8.97	70.8 g	Benign	Malignant	
642B				Benign	Malignant	
642E				Benign	Malignant	
643D	62	11	NR	Benign	Malignant	
645C	62	4.7	41 g	Benign	Benign	
647B	55	7.7	52 g	Benign	Malignant	
647D				Benign	Benign	
647F				Benign	Benign	
650A	78	7.96	47 g	Benign	Benign	
650B				Benign	Benign	
650D				Benign	Malignant	
650E				Benign	Malignant	
732B	66	6.55	23 g	Benign; PTM	Malignant	
733B	64	8.1	35 g	Benign; PTM	Malignant	
733E				Benign; PTM	Malignant	
735E	76	9.66	65	Benign; PTM	Benign	
735F				Benign; PTM	Benign	
736B	68	8.8	29 g	Benign	Benign	
736E				Benign	Benign	
776A	65	7.7	81 g	Benign; PTM	Malignant	
776C				Benign	Benign	
776E				Benign	Benign	
777A	53	4.55	NR	Benign	Benign	
777B				Benign	Malignant	
777C				Benign	Malignant	
777D				Benign	Malignant	
777E				Benign	Benign	
778E	57	83.5	98 g	Benign	Benign	
787A	75	NR	NR	Benign	Benign	
805F	72	8.3	24 g	Benign; PTM	Malignant	
807F	76	4.35		Benign; PTM	Malignant	
809B	73	16.5	NR	Benign	Benign	

A subset of nucleic acids extracted from serial prostate needle biopsy specimens, included in the confirmation study, was submitted to the Biochemical Science Division of the National Institute of Standards and Technology (NIST) for analytic cross-validation under the National Cancer Institute Early Detection Research Network program. The standard operating procedures developed and used at Genesis Genomics (GGI) were followed.

All samples had known Cts (from work done at GGI) and were blinded to NIST scientists. These samples consisted of 46 benign, 41 PTM, and 25 malignant cores. NIST results demonstrated a sensitivity of 83% and a specificity of 79%, very close to the results obtained at GGI. Likewise, the area under the ROC curve was 0.87 **Figure 5A**, in comparison with 0.83 for GGI data. **Figure 5B** depicts the mean Cts and 95% CI for the NIST study.

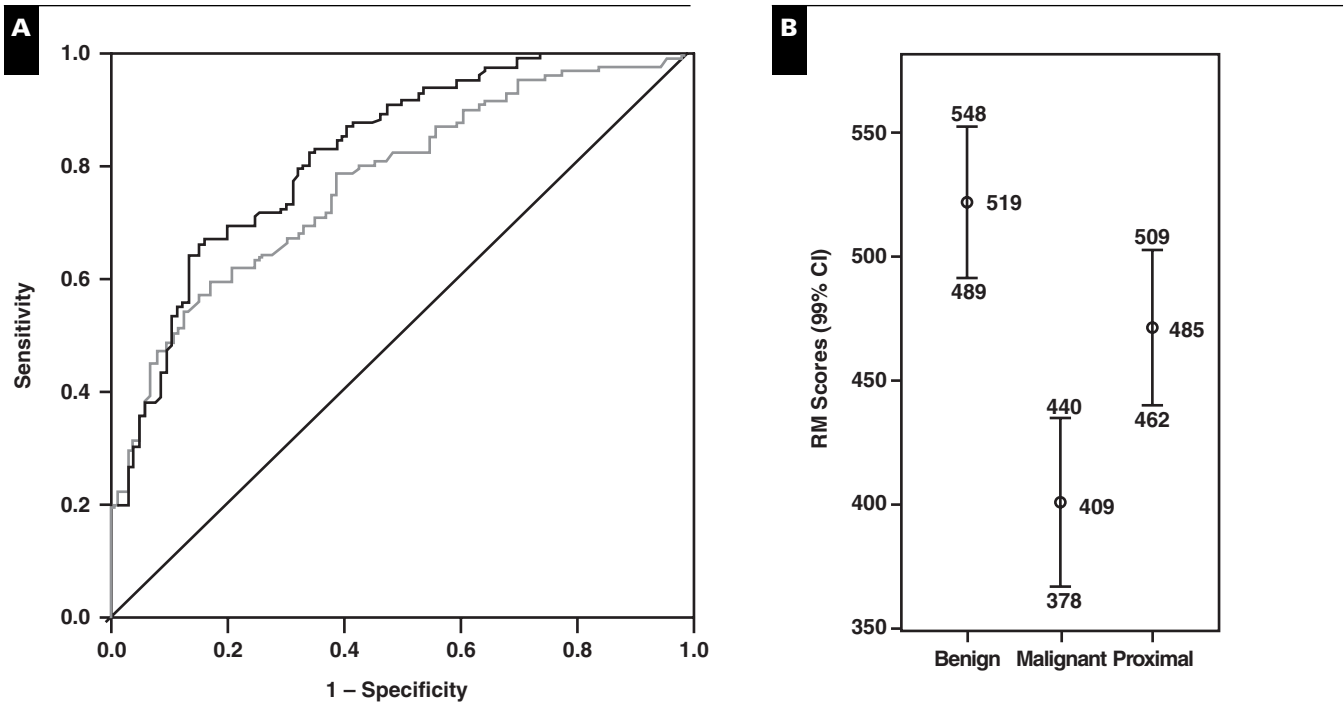


Figure 4 **A**, A receiver operating characteristic curve for the deletion cycle thresholds and residual mitochondrial DNA (RM) scores computed with reference to histopathology for benign and malignant samples indicates good performance of the deletion alone and the RM scores in discriminating benign from malignant biopsy specimens. Area under the curve: black, 3.4-kb mitochondrial genome deletion (3.4mtΔ) cycle thresholds, 0.83; gray, RM scores, 0.77. **B**, The 3.4mtΔ is reproduced in a larger study. The RM scores and 99% confidence interval (CI) for benign, malignant, and proximal samples for the confirmation studies are plotted.

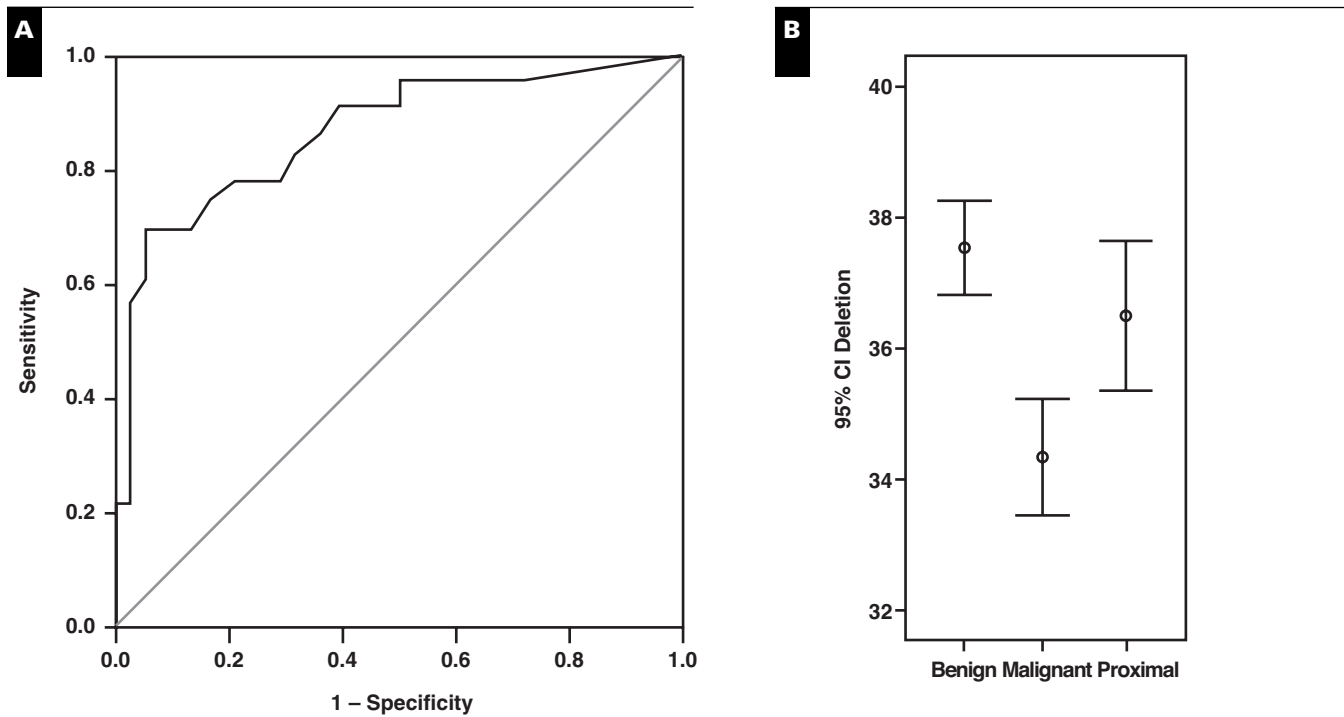


Figure 5 The receiver operating characteristic curve (**A**; area under the curve, 0.87) and mean cycle thresholds and 95% confidence interval (CI) (**B**) of the external validation study at the National Institute of Standards and Technology/Early Detection Research Network demonstrate that the 3.4-kb mitochondrial genome deletion is reproducible in identifying prostate cancer.

Discussion

Previously, our group studied the accelerated mutation rate of the mtgenome within the malignant prostate.¹¹ Briefly, malignant, adjacent, and distant benign samples were used. These histologic tissue types were captured from 24 prostatectomy samples by using laser capture microdissection. Complete mtgenome sequencing was attempted on all samples. In comparison with results from benign samples, representing people with moderately high PSA values and negative biopsy reports, results demonstrated an accelerated but equal mtgenome somatic mutation rate in all tissues recovered from a malignant prostate gland. This finding suggests that underlying molecular alterations are apparent in normal-appearing tissue, before visual morphology, indicative of malignant transformation. We continued this work by screening for large-scale mtgenome deletions in PCa. The mtDNA deletions are known to be associated with many cancers. The objective was to locate a simple deletion biomarker that can discriminate benign from malignant prostate tissue.

The pilot and confirmation studies demonstrated that the 3.4mt Δ is a highly significant biomarker for PCa ($P < .0001$) in comparison with histopathologic examination. To determine if the malignant transformation process was underway and discernible at the molecular level within “normal” prostate tissue, visually normal glandular tissue in proximity to a malignant lesion (PTM) was characterized for the 3.4mt Δ . Malignant and PTM biopsy samples for the pilot study were procured from cases after consulting the associated prostatectomy pathology report. This facilitated tight control over the selection of PTM samples. Moreover, the size and extent of the malignant lesion were known. Finally, benign samples were chosen on the basis of a single negative biopsy result.

Criteria for the confirmation studies were slightly different because the samples were taken from several urologic clinics. This was intended to model the use of biopsy samples procured directly from clinics; therefore, it was impossible to determine the exact location of negative tissue in respect to tumor because patients were recruited before treatment was finalized. Only the general anatomic location of the biopsy was known. Finally, to ensure the negative status of benign samples, the first of at least 2 successive benign biopsy procedures was used.

Irrespective of these parameter variations between the pilot and confirmation studies, both results supported a prostate field cancerization. This is reflected in the clustering of the PTM samples. If there is a field cancerization, the PTM samples should cluster with the malignant samples or intermediately between the malignant and benign samples. Interestingly, the mean of the well-defined location of the proximal samples selected in the pilot study cannot be statistically resolved from the mean of the malignant grouping. In

contrast, the PTM samples of the confirmation study resolved into an intermediate position between the benign and malignant categories. The 99% CI of this grouping does not overlap with that of the malignant samples. Furthermore, the confirmation study demonstrated a tighter cluster of the benign samples, in comparison with the pilot study, which might be due to the larger benign sample size used in the confirmation study, resulting in a smaller CI. In addition, the strict criteria used to define benign samples for the confirmation study should exclude biopsy specimens that may be found malignant on a second procedure. Furthermore, in both studies, the 99% CIs of the PTM overlapped slightly with the benign interval, suggesting that some of these samples are actually benign and uninfluenced by the cancerization field effect. This might be a function of the size of this field or may indicate the directional spread of a tumor. These aspects, however, require further study. It is important to note that the marker seems unaffected by common benign prostate conditions.

Field cancerization was first described in 1953 by Slaughter and colleagues (reviewed by Dakubo et al¹⁸). More recently, molecular field cancerization has been described for several cancers, including gastric, breast, head and neck, colorectal, acute promyelocytic and chronic myeloid leukemia, larynx, pancreas, bladder, and lung cancers.¹⁸ In PCa, field cancerization has been described for genomic instability and gene expression profiles. With regard to the 3.4mt Δ , additional studies are required to determine the extent and significance of this field cancerization in PCa. This has important implications for “clean” tumor margins based on histopathologic examination because it is well known that molecular markers can more accurately determine actual disease-free margins. Finally, is this effect present before malignant transformation, and if so, can it be used for risk assessment and early detection of PCa? These issues are the subject of continuing studies.

A useful biomarker in the management of PCa will be one that not only detects the disease but also behaves as a biosensor of premalignant and suspicious lesions indicative of disease progression. As well, a biomarker that predicts tumor behavior (indolent vs aggressive tumors) will tremendously aid patient management. Future studies of this biomarker, using laser-capture microdissection, will address the preceding questions. Whereas the present molecular data do not tremendously advance the management of PCa, they have some usefulness in early detection of the disease. First, a positive result will prompt early rather than late rebiopsy. Second, a positive anatomic site will indicate an area where a lesion is possibly present and, therefore, requires special attention on rebiopsy.

*From*¹*Genesis Genomics, Thunder Bay, Canada; the Departments of*²*Pathology and Laboratory Medicine, Mount Sinai Hospital, Toronto;* ³*Pathology and* ⁴*Urology, Thunder Bay Regional Health Sciences Centre, Thunder Bay;* ⁵*Pathology and Laboratory*

Medicine, University of Minnesota, Duluth; and ⁶Laboratory Medicine, VA Medical Center Research Service, Minneapolis, MN; the ⁷National Institute of Standards and Technology, Biochemical Science Division, Gaithersburg, MD; ⁸Cipher Systems, Crofton, MD; and ⁹Division of Cancer Prevention, National Cancer Institute, Rockville, MD.

Financial support for this project was provided to Genesis Genomics by Industry Canada (FedNor), Sudbury, Canada, and Northern Ontario Heritage Fund Corporation (NOHFC), Sault Ste Marie, Canada. Funding was also provided for this study by an interagency agreement (Y1CN5001-01) between the National Institute of Standards and Technology and the National Cancer Institute.

Address reprint requests to Dr Parr: Genesis Genomics, 1000-290 Munro St, Thunder Bay, Ontario, Canada, P7A 7T1.

Acknowledgments: We thank the patients and their physicians for participation in this study and William Montelpare, PhD, for helping with statistical analysis.

Disclaimer: Certain commercial equipment, instruments, materials, or companies are identified in this article to specify adequately the experimental procedure. Such identification does not imply recommendation or endorsement by the National Institute of Standards and Technology, nor does it imply that the materials or equipment identified are the best available for the purpose.

* These authors work for and own stock options in Genesis Genomics.

References

- Lee WK, Thevenod F. A role for mitochondrial aquaporins in cellular life-and-death decisions? *Am J Physiol Cell Physiol*. 2006;291:C195-C202.
- Singh KK. Mitochondria damage checkpoint in apoptosis and genome stability. *FEMS Yeast Res*. 2004;5:127-132.
- Brenner C, Kroemer G. Apoptosis: mitochondria; the death signal integrators. *Science*. 2000;289:1150-1151.
- Arakaki N, Nishihama T, Owaki H, et al. Dynamics of mitochondria during the cell cycle. *Biol Pharm Bull*. 2006;29:1962-1965.
- Modica-Napolitano JS, Singh KK. Mitochondria as targets for detection and treatment of cancer. *Expert Rev Mol Med*. 2002;4:1-19.
- Van Houten B, Woshner V, Santos JH. Role of mitochondrial DNA in toxic responses to oxidative stress. *DNA Repair (Amst)*. 2006;5:145-152.
- DiMauro S, Schon EA. Mitochondrial respiratory-chain diseases. *N Engl J Med*. 2003;348:2656-2668.
- Carew JS, Huang P. Mitochondrial defects in cancer. *Mol Cancer*. 2002;1:9.
- Parr RL, Dakubo GD, Thayer RE, et al. Mitochondrial DNA as a potential tool for early cancer detection. *Hum Genomics*. 2006;2:252-257.
- Chen JZ, Gokden N, Greene GF, et al. Extensive somatic mitochondrial mutations in primary prostate cancer using laser capture microdissection. *Cancer Res*. 2002;62:6470-6474.
- Parr RL, Dakubo GD, Crandall KA, et al. Somatic mitochondrial DNA mutations in prostate cancer and normal appearing adjacent glands in comparison to age-matched prostate samples without malignant histology. *J Mol Diagn*. 2006;8:312-319.
- Brandon MC, Lott MT, Nguyen KC, et al. MITOMAP: a human mitochondrial genome database: 2004 update. *Nucleic Acids Res*. 2005;33:D611-D613.
- Jessie BC, Sun CQ, Irons HR, et al. Accumulation of mitochondrial DNA deletions in the malignant prostate of patients of different ages. *Exp Gerontol*. 2001;37:169-174.
- Higuchi M, Kudo T, Suzuki S, et al. Mitochondrial DNA determines androgen dependence in prostate cancer cell lines. *Oncogene*. 2006;25:1437-1445.
- Gomez-Zaera M, Abril J, Gonzalez L, et al. Identification of somatic and germline mitochondrial DNA sequence variants in prostate cancer patients. *Mutat Res*. 2006;595:42-51.
- Djavan B, Milani S, Remzi M. Prostate biopsy: who, how and when: an update. *Can J Urol*. 2005;12:44-48.
- Heaphy CM, Bisoffi M, Fordyce CA, et al. Telomere DNA content and allelic imbalance demonstrate field cancerization in histologically normal tissue adjacent to breast tumors. *Int J Cancer*. 2006;119:108-116.
- Dakubo GD, Jakupciak JP, Birch-Machin MA, et al. Clinical implications and utility of field cancerization. *Cancer Cell Int*. 2007;7:2.